Chemical conversion of human fibroblasts into functional schwann cells

Thoma, Eva C; Merkl, Claudia; Heckel, Tobias; Haab, Rachel; Knoflach, Frederic; Nowaczyk, Corinne; Flint, Nicholas; Jagasia, Ravi; Jensen Zoffmann, Sannah; Truong, Hoa Hue; Petitjean, Pascal; Jessberger, Sebastian; Graf, Martin; Iacone, Roberto

Abstract: Direct transdifferentiation of somatic cells is a promising approach to obtain patient-specific cells for numerous applications. However, conversion across germ-layer borders often requires ectopic gene expression with unpredictable side effects. Here, we present a gene-free approach that allows efficient conversion of human fibroblasts via a transient progenitor stage into Schwann cells, the major glial cell type of peripheral nerves. Using a multikinase inhibitor, we transdifferentiated fibroblasts into transient neural precursors that were subsequently further differentiated into Schwann cells. The resulting induced Schwann cells (iSCs) expressed numerous Schwann cell-specific proteins and displayed neurosupportive and myelination capacity in vitro. Thus, we established a strategy to obtain mature Schwann cells from human postnatal fibroblasts under chemically defined conditions without the introduction of ectopic genes.

Stem Cell Reports

Report

Chemical Conversion of Human Fibroblasts into Functional Schwann Cells

Eva C. Thoma,[1,*] Claudia Merkl,[1,3] Tobias Heckel,[1] Rachel Haab,[1] Frederic Knoflach,[1] Corinne Nowaczyk,[1] Nicholas Flint,[1] Ravi Jagasia,[1] Sannah Jensen Zoffmann,[1] Hoa Hue Truong,[1] Pascal Petitjean,[1] Sebastian Jessberger,[2] Martin Graf,[1] and Roberto Iacone[1]

[1]Roche Pharma Research and Early Development, Roche Innovation Center Basel, 4070 Basel, Switzerland
[2]Brain Research Institute, Faculty of Medicine and Science, University of Zurich, 8057 Zurich, Switzerland
[3]Present address: Novartis Pharma AG, Novartis Institutes for BioMedical Research, Musculoskeletal Diseases, 4056 Basel, Switzerland
*Correspondence: eva_christina.thoma@roche.com
http://dx.doi.org/10.1016/j.stemcr.2014.07.014
This is an open access article under the CC BY-NC-ND license (http://creativecommons.org/licenses/by-nc-nd/3.0/).

SUMMARY

Direct transdifferentiation of somatic cells is a promising approach to obtain patient-specific cells for numerous applications. However, conversion across germ-layer borders often requires ectopic gene expression with unpredictable side effects. Here, we present a gene-free approach that allows efficient conversion of human fibroblasts via a transient progenitor stage into Schwann cells, the major glial cell type of peripheral nerves. Using a multikinase inhibitor, we transdifferentiated fibroblasts into transient neural precursors that were subsequently further differentiated into Schwann cells. The resulting induced Schwann cells (iSCs) expressed numerous Schwann cell-specific proteins and displayed neurosupportive and myelination capacity in vitro. Thus, we established a strategy to obtain mature Schwann cells from human postnatal fibroblasts under chemically defined conditions without the introduction of ectopic genes.

INTRODUCTION

In recent years, the idea of directly converting one somatic cell type into another has attracted substantial attention because it offers a valuable source for cells that are difficult to access (Vierbuchen and Wernig, 2011). However, a major drawback linked to current strategies is the fact that they are based on ectopic expression of key developmental genes that often have to be stably integrated into the genome. Despite the possibilities to tightly control ectopic gene expression, such genetic modifications may have undesired effects. Small molecules specifically modifying key signaling pathways provide a powerful tool to enhance conversion or even replace reprogramming genes. Recently, the generation of pluripotent stem cells in mouse by small molecules has been reported (Hou et al., 2013). However, chemical conversion of human cells has thus far only been demonstrated for the generation of endodermal cells (Pennarossa et al., 2013).

Here, we aimed to convert human fibroblasts into Schwann cells, the major glial cell type of the peripheral nervous system.

Using a multikinase inhibitor, we attempted to convert fibroblasts first into a transient precursor stage showing features of neural crest, the origin of Schwann cells. These transient precursors were then further differentiated into mature Schwann cells. Importantly, the complete cell conversion process did not require the expression of ectopic genes but was solely based on chemical treatment. It thus represents a promising approach to generate patient-specific Schwann cells and proves that cellular identities can be significantly altered by small molecule treatment.

RESULTS

Identification of a Compound Allowing Neural Transdifferentiation

Current protocols for converting one cell type into another often suffer from low efficiencies (Table S1 available online). This might be partially due to the fact that many protocols attempt to obtain postmitotic cell types, e.g., neurons. Thus, the conversion procedure includes a stop of proliferation, which reduces both yield and efficiency. To maximize these parameters, we established a two-step protocol for fibroblast transdifferentiation. First, fibroblasts are converted into a transient, proliferative neural precursor stage. In a second step, these precursors are differentiated into induced Schwann cells (iSCs).

In vivo, Schwann cells arise from the neural crest (NC), a multipotent, neuroepithelial cell population that is specified by numerous signaling cues (Stuhlmiller and García-Castro, 2012). We reasoned that the combination of neural inductive cues together with NC specifiers might induce a NC fate in fibroblasts. As potent neural inducing signal we used a small molecule—compound B (CB)—that had been identified in a high-throughput screen to selectively promote proliferation of neural stem cells while inhibiting their differentiation (Figures 1A–1C). Induction of a proliferative precursor stage in fibroblasts was analyzed by the capacity of sphere formation, an assay widely used to identify cells with progenitor features (Dontu et al., 2003; Tropepe et al., 2000). CB treatment resulted in a significant increase in both sphere size and total cell number (Figure 1D) compared to control-treated cells. Kinase profiling identified CB as potent multikinase inhibitor with the
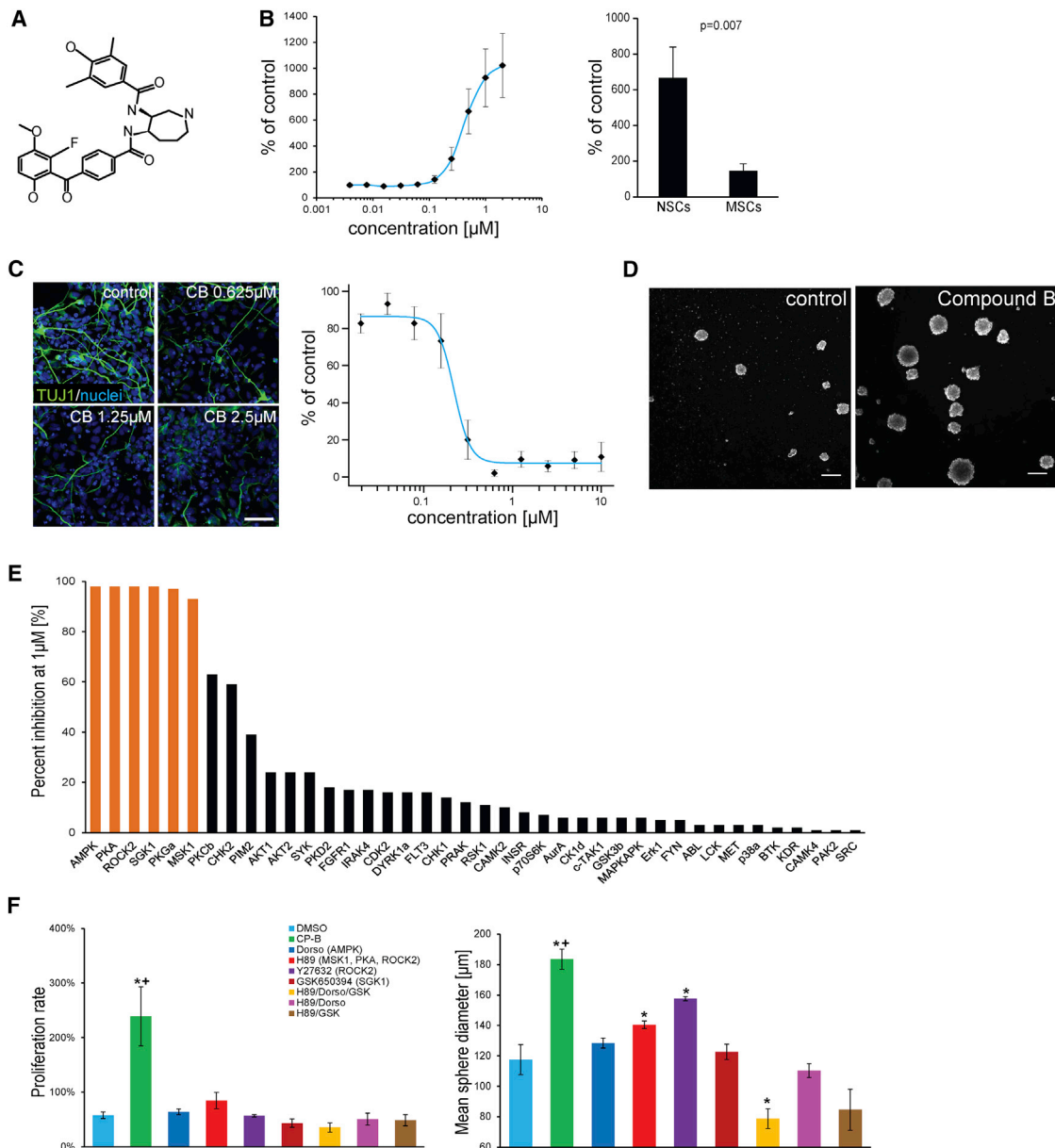
Figure 1. Identification of a Small Molecule Enhancing Neural Stem Cell Proliferation and Enabling Conversion of Fibroblasts into Neurosphere-like Structures

(A) Structure of compound B (CB).

(B) CB selectively promotes proliferation of ESC-NSCs. Proliferation was analyzed by ATP assay. Fold increase to control-treated cells is shown. Left: dose-response assay with ESC-NSCs (n = 4). Right: effect of CB (0.5 μM) on proliferation of ESC-NSCs (n = 4) and ESC-MSCs (n = 2).

(C) CB inhibits differentiation of ESC-NSCs in a dose-dependent manner. Left: immunostaining of TUJ1 of NSCs treated for 7 days with DMSO (control) or CB at various concentrations. Scale bar, 100 μm. Right: quantification of total length of neurite network upon CB treatment for 7 days. Values are normalized to control-treated cells (n = 3).

(D) CB (2 μM)-treated fibroblasts form sphere-like structures in suspension. Scale bars, 200 μm.

(E) Kinase selectivity profiling of CB. Orange bars represent kinases inhibited more than 80% at 1 μM.

(F) Single or combined inhibition of CB target kinases by other compounds (targets in parentheses) has no or smaller effect on sphere formation. Graphs show proliferation rate as fold change of initial cell number (left) and mean sphere diameter (right) at day 3 of suspension culture (n = 3). *p < 0.05 compared to DMSO control. +, p < 0.05 for CB compared to single inhibitors.

major targets AMPK, PKA, MSK1, SGK1, ROCK2, and PKGa (Figure 1E). Single inhibitors of these kinases or combinations of inhibitors did not induce similar increase in sphere size and cell number as CB (Figure 1F). However, compounds H89 and Y27632, both inhibiting ROCK2, also induced a significant increase in sphere diameter compared to control-treated cells but did not induce an increase in proliferation rate. Thus, the effects of CB on sphere formation and cell proliferation apparently depend on the inhibition of a combination of distinct signaling pathways.

Conversion of Fibroblasts into Transient Neural Precursors

Based on sphere formation as initial step, we established an optimized protocol to induce a transient precursor (tP) phenotype in postnatal fibroblasts (Figure 2A) tested negative for neural crest and Schwann cell markers (Figures S1A–S1C). First, fibroblasts were treated with the histone deacetylase (HDAC) inhibitor valproic acid (VPA). VPA is known to enhance reprogramming and transdifferentiation processes (Huangfu et al., 2008; Tursun et al., 2011) and increased the effect of CB on sphere size in our protocol (Figure 2B). VPA treatment was followed by induction of a neural precursor fate by CB treatment in neural stem cell medium. The resulting cells were expanded and additionally treated with synergistic inhibitors of BMP (Noggin), TGF-β (SB431542), and GSK3β (CP21, Roche Compound) signaling. This strategy is known to enhance gene-transfer-dependent neural conversion of fibroblasts (Ladewig et al., 2012). Then, spheres were plated on polyornithine-laminin (POL) and transferred to differentiation medium. Sphere attachment was observed within 2 hr after plating, and cells soon started to migrate out of spheres. In contrast, if spheres had been generated using inhibitors of single CB targets, sphere attachment was highly impaired and no or only poor migration of cells was observed (Figure S2). During physiological NC development, laminin represents one of the key ECM components mediating migration and survival of NC cells (Bronner-Fraser, 1986; Desban et al., 2006). Thus, the capacity to attach rapidly and migrate on laminin indicates that CB-treated cells have adopted some NC features.

Twenty-four hours after attachment, cells stained positive for neuroepithelial markers SOX1 and NESTIN but did not express neural crest markers. No expression of SOX2 was observed indicating the absence of neural stem cells (Figure 2C). One week later (d18), cells expressed neural crest markers CD271, SNAI1, SOX10, FOXD3, and PAX3 suggesting they had adopted some features of NC cells (Figures 2D and 2E). Loss of fibroblast identity was indicated by downregulation of the fibroblast surface marker CD29 (Figure 2E). When cultured in specific differentiation media, tPs formed adipocytes, smooth muscle cells, and chondrocytes suggesting a multipotent differentiation capacity (Figures 2F–2H). To exclude the possibility that the induced tPs originated from rare mesenchymal stem cells (MSCs) in the initial fibroblasts, we tested both fibroblasts and tPs for expression of the MSC marker CD146 (Halfon et al., 2011). No CD146-positive cells were detected in the initial fibroblast population or in tPs (Figures S1D and S1E).

Differentiation into Induced Schwann Cells

To induce Schwann cell formation, tPs were cultured in differentiation medium for 3–4 weeks. After an initial proliferation phase during the tP stage, cell numbers decreased about 50% and then remained constant until the end of the experiment (Figure S3A). After 4 weeks, cells expressed Schwann cell markers PLP, EGR2 (also known as KROX20), S100B, GALC, and GFAP (Figures 3A–3E, S3B, and S3C) (Bhatheja and Field, 2006; Jessen and Mirsky, 2005). Quantification of cells expressing the Schwann cell marker PLP (Griffiths et al., 1995; Kamholz et al., 1992) revealed that more than 60% of cells had transdifferentiated into induced Schwann cells (iSCs) (Figure 3E). Cells stained negative for the fibroblast marker HMMR and the neuron marker MAP2 indicating the absence of fibroblast and neurons, respectively (Figures S3D and S3E).

To analyze the conversion process on the molecular level, genome-wide gene expression profiling was performed at different time points and with primary Schwann cells. Principal component analysis (PCA) revealed a clear difference between fibroblasts and tPs on the one hand and primary and induced Schwann cells on the other hand, which are more similar to each other than to fibroblasts (Figure 3F). This similarity of primary to induced Schwann cells is also reflected by the high Pearson correlation coefficient for all expressed genes (r = 0.93). Gene set enrichment analysis (GSEA) revealed significant upregulation of several biological processes corresponding to Schwann cell functions like extracellular matrix organization, NCAM signaling for neurite outgrowth, Notch signaling, or immune response signaling pathways (Figure 3G; Table S2) (Kidd et al., 2013). These networks were also activated in primary Schwann cells further supporting the Schwann cell identity of iSCs (Table S2). In addition, gene expression profiling showed that iSCs produced several neurotrophic factors for neuronal survival, regeneration, and axonal outgrowth (Figure S3H) (Raivich and Makwana, 2007). Gene sets associated with mitotic cell division were downregulated, which is consistent with the transition from proliferative fibroblasts and precursors into postmitotic Schwann cells (Figures 3G and S3G; Table S2).

It has been shown that so-called skin-derived precursors (Toma et al., 2005) show NC stem cell properties and can give rise to Schwann cells (Fernandes et al., 2004; McKenzie
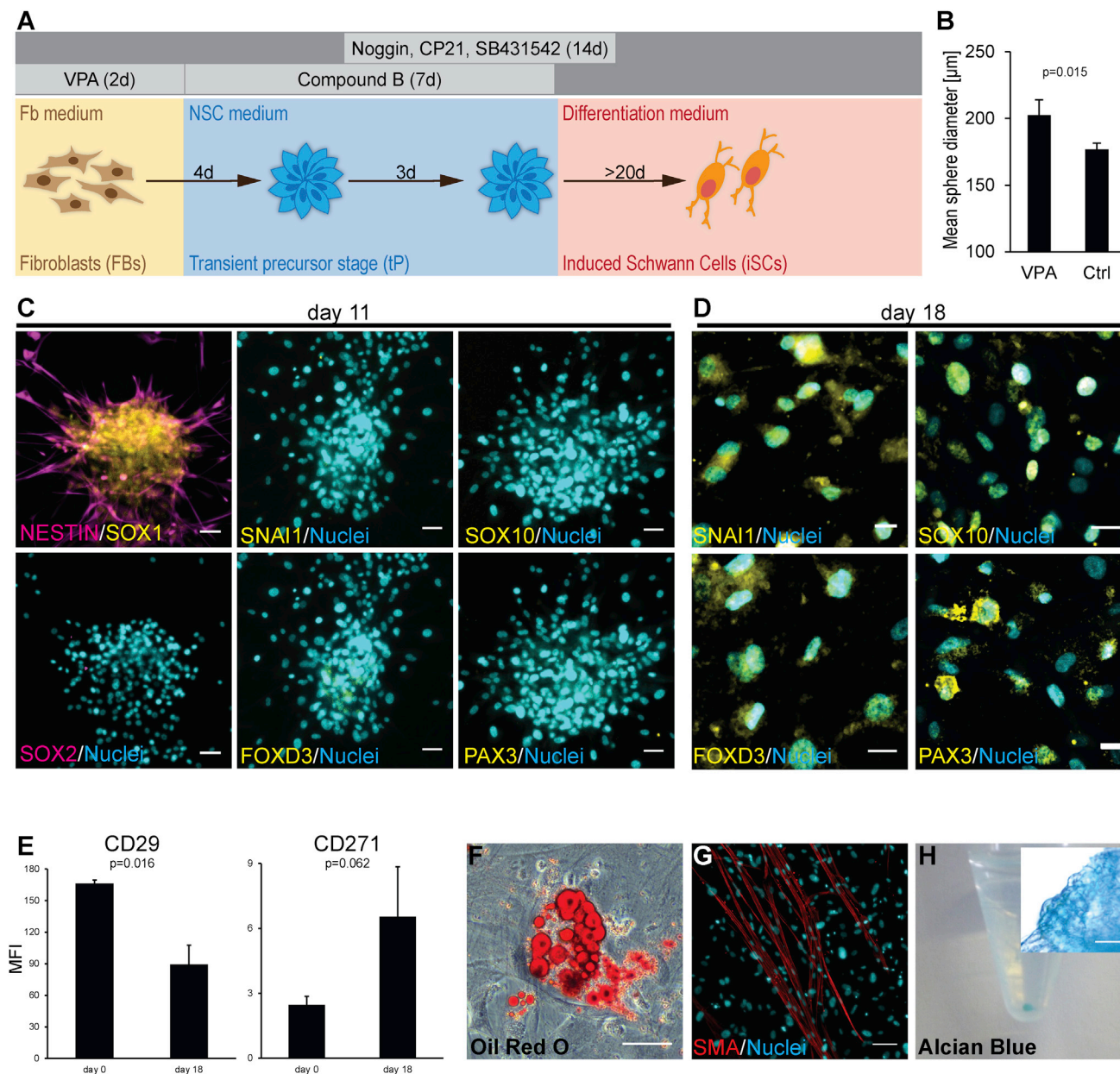
Figure 2. Conversion of Human Fibroblasts into a Transient Neural Precursor Stage

(A) Scheme of experimental setup for conversion into induced Schwann cells.

(B) Pretreatment with valproic acid (VPA) results in increased sphere size. Columns show mean sphere diameter ± SD at day 3 of suspension culture (n = 4).

(C) Secondary spheres at day 11 with bipolar cells growing out of spheres. Cells express neural plate markers SOX1 and NESTIN (top left). No expression of NSC marker SOX2 and of neural crest markers SNAI1, SOX10, FOXD3, and PAX3 was detected. Scale bars, 50 μm.

(D) At day 18, cells express neural crest markers SNAI1, SOX10, FOXD3, and PAX3. Scale bars, 20 μm.

(E) Flow cytometry of precursors (d18) and fibroblasts (d0) revealed downregulation of fibroblast marker CD29 and upregulation of neural crest marker CD271. Panels show quantification of mean fluorescence intensity (MFI) (n = 3).

(F–H) Nonneural differentiation of transient precursors. (F) Adipocyte formation analyzed by oil red O staining. (G) Formation of SMA+ smooth muscle cells. (H) Formation of chondrocytes analyzed by Alcian blue staining. Inset shows closeup of chondrogenic pellet. Scale bars, 50 (F), 100 (G), and 20 μm (H, inset).
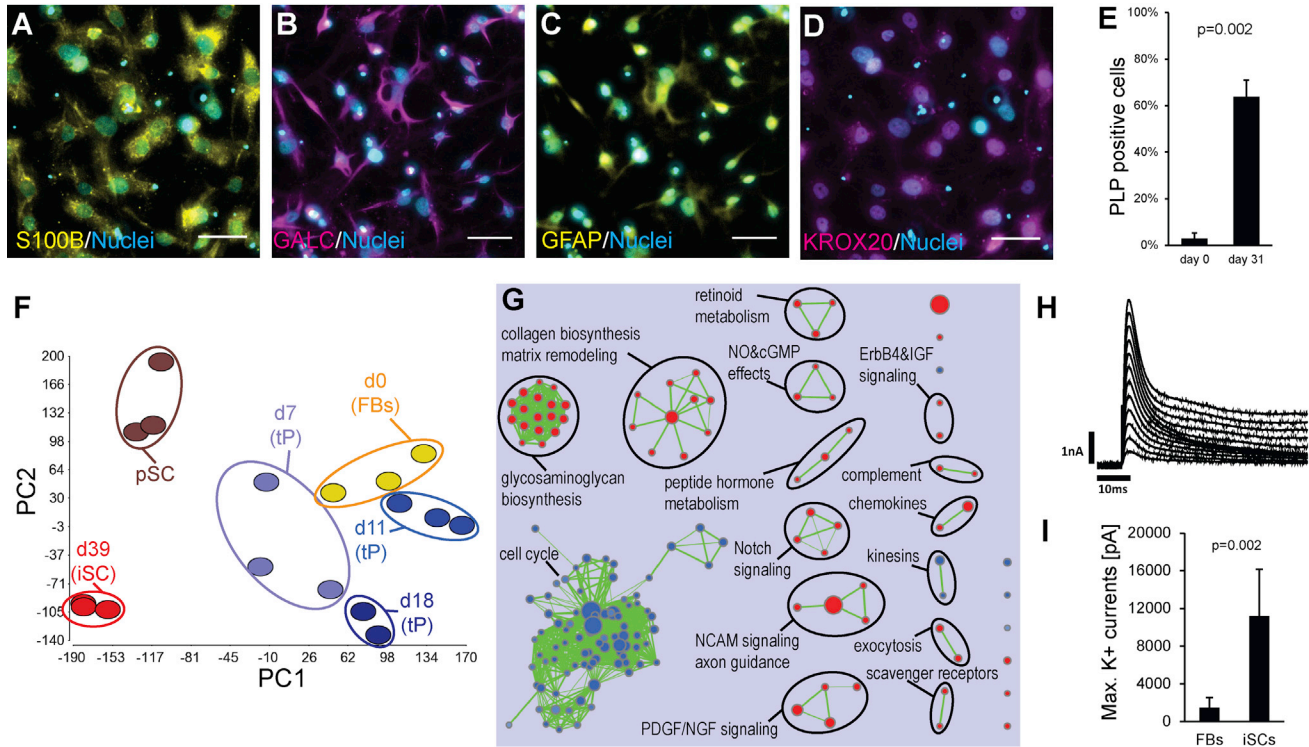
See also Figure S1 and S2.

Figure 3. Differentiation of Transient Precursors into Induced Schwann Cells

(A–D) iSCs express Schwann cell markers. Scale bars, 50 μm.

(E) Quantification of PLP-positive cells at d31. Few PLP-positive fibroblasts are due to background signal (n = 3).

(F) Principal component analysis of whole-transcriptome expression profiles from fibroblasts (d0), transdifferentiated cells at d7 (early tP), d11 (early tP), d18 (late tP), d39 (iSCs), and primary Schwann cells (pSCs). Principal component 1 (x axis) accounts for 27.4% and principal component 2 (y axis) accounts for 16.5% of the variation of the data set. Each stage is represented by at least two data points derived from independent experiments. The clustered transcriptomic profiles at day 39 suggest the robustness of the protocol.

(G) Enrichment map of gene sets for cellular signaling pathways (Reactome/NCI Nature PID) derived from GSEA comparing iSCs (d39) with fibroblasts (d0). Red nodes represent gene sets enriched in iSCs, whereas blue nodes represent gene sets enriched in fibroblasts. Nodes are grouped and annotated by their similarity according to related gene sets. Cluster of functionally related nodes were summarized and annotated using WordCloud (n = 3).

(H) Whole patch-clamp analysis of iSCs. Voltage-dependent current obtained from a −70 to +40 mV in 10 mV increasing steps protocol from a holding potential Vh = −80 mV. Absence of early inward current confirms the deficiency of voltage-dependent Na^+ channels, whereas the outward component is consistent with the presence of voltage-dependent K^+ channels.

(I) Maximal voltage-dependent K^+ currents are significantly higher in iSCs than in fibroblasts. Columns show means ± SD of different cells (FBs: n = 12; iSCs: n = 7) measured in two independent experiments.

See also Figure S3 and Table S2.

---

et al., 2006). To exclude that iSCs originated from skin-derived precursors, depletion of CD271-positive cells was performed in the initial fibroblast population using MACS. CD271-depleted fibroblasts converted into tPs and further into iSCs with no difference in time course or efficiency compared to unsorted fibroblasts (Figures S3I–S3Q). These results suggest that indeed iSCs originated from fibroblasts that converted toward another phenotype, albeit the possibility that rare skin-derived precursors differentiated into Schwann cells cannot be completely excluded.

Functional Features of Induced Schwann Cells

To analyze iSC functionality, we first tested excitability of iSCs performing whole patch-clamp recordings. Brief depolarizing current pulses of increasing intensity did not evoke action potentials. However, upon 100 ms voltage-step pulses from −70 to +40 mV in 10 mV steps increments, a sustained outward current component was observed indicating the presence of voltage-dependent K^+ channels, a known feature of Schwann cells (Baker, 2002). K^+ currents were significantly larger in iSCs compared to untreated fibroblasts (Figures 3H, 3I, and S3F).
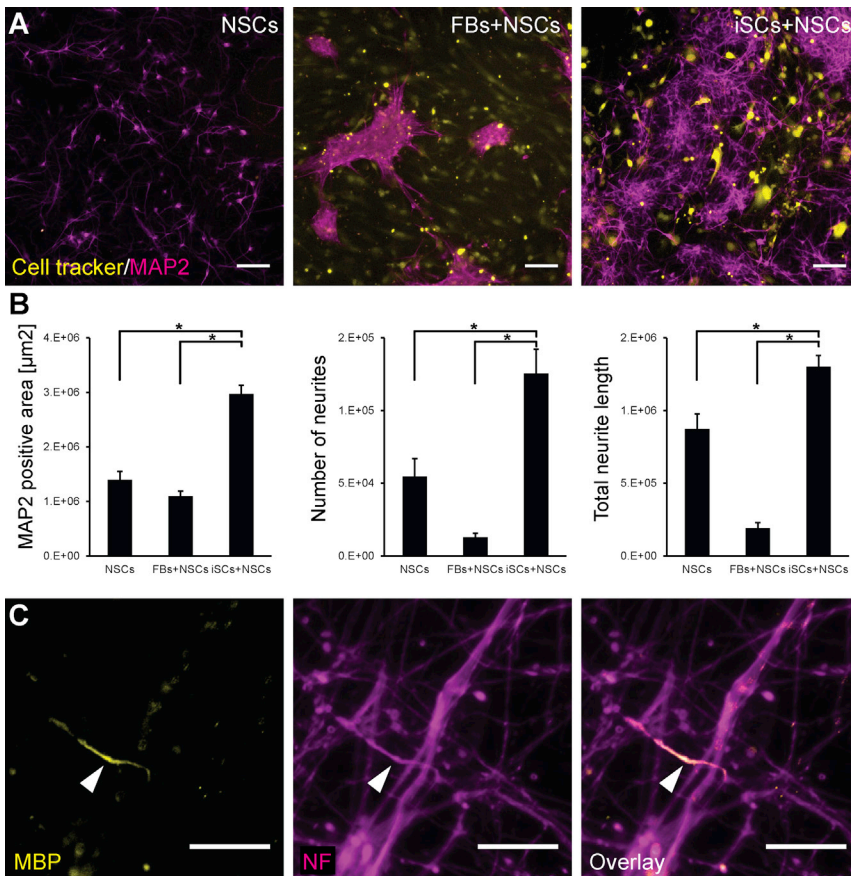
Figure 4. Functionality of iSCs in Coculture with Neuronal Cells

(A) Culture of NSC-derived neurons alone, on cell tracker-labeled fibroblasts and iSCs, respectively. Scale bars, 100 μm.

(B) NSC-neurons cultured with iSCs form a more dense and branched network analyzed by MAP2-stained area, neurite number, and total neurite length (n = 3). *p < 0.05.

(C) Coculture of iSCs with primary rat DRG neurons. Some iSCs form single myelinated fragments (arrowhead) detected by colocalization of MBP staining (yellow) and neurofilament (NF) staining (magenta). Scale bars, 20 μm.

See also Figure S4.

To analyze neuroprotective functionality of iSCs, cells were cocultured with neurons differentiated from human embryonic stem cell (ESC)-derived neural stem cells (NSC-neurons). As control, NSC-neurons were plated on POL or untreated fibroblasts. NSC-neurons plated on fibroblasts aggregated in dense clusters whereas cocultured iSCs and NSC-neurons formed a dense, multicellular network (Figures 4A and S4). MAP2 staining confirmed that NSC-neurons cultured with iSCs formed a more branched neurite network than NSC-neurons grown alone or with fibroblasts (Figure 4B). Moreover, total number of neurons was also increased in coculture with iSCs (Figure S4J). These results suggest that iSCs are capable to enhance neuronal survival, differentiation, and neurite network formation.

To test if iSCs are capable of myelination, iSCs were cocultured with primary rat dorsal root ganglia neurons (DRGs). After 3 weeks, myelinated axon segments could be observed further confirming the functionality of iSCs (Figure 4C). The low frequency of myelinated fragments (five to ten fragments/96 well) might be due to species differences between iSCs and neurons. This observation is in line with previous studies showing that human Schwann cells had a markedly reduced efficacy to myelinate rat sen-

sory neurons compared to primary rat Schwann cells (Lehmann et al., 2012).

DISCUSSION

In recent years, numerous studies reporting reprogramming or transdifferentiation of somatic cells have shown that even in terminally differentiated cells fate plasticity can be evoked and that transition to other cell types, even across germ-layer boundaries, is still possible.

Here, we present an approach to transdifferentiate human fibroblasts via a transient precursor stage into Schwann cells that does not depend on ectopic gene expression but is based on chemical modification of defined signaling pathways. Such gene-free, chemical-based conversion strategies allow the generation of cells without genetic modifications and furthermore can be very tightly controlled by altering concentrations or duration of small molecule treatment.

In our approach, conversion to Schwann cells was induced by sequential treatment with defined compounds. First, a brief VPA treatment step probably resulted in an

erase of epigenetic signatures making cells more amenable for cell-fate changing signals—a process that may also be involved in gene-free iPS generation or transdifferentiation into endodermal cells (Hou et al., 2013; Pennarossa et al., 2013). Fate determination toward transient precursors was achieved by treatment with CB inhibiting AMPK, MSK1, PKA, ROCK2, PKGa, and SGK1. Several studies of these signaling pathways allow assumptions regarding the mechanistic regulation of the conversion process. Because upregulation of SGK1 correlates with cell death in neurodegenerative disease (Schoenebeck et al., 2005), its inhibition might enhance the survival of cells that converted toward a neural fate. Moreover, CB might abolish a metabolic barrier mediated by AMPK signaling, which is known to prevent reprogramming processes (Vazquez-Martin et al., 2012).

ROCK2 inhibition evokes a proliferative, stem cell-like phenotype (Terunuma et al., 2010), promotes emigration of neural crest cells (Groysman et al., 2008), and has neuroprotective effects (Ding et al., 2009). These effects might also support fibroblast conversion into neural precursors and iSCs.

Additionally, our approach included small molecule-based inhibition of TGF-β, BMP, and GSK3 signaling, a strategy known to direct differentiation of ESCs to neuroepithelial and/or neural crest fates (Chambers et al., 2009; Menendez et al., 2011).

Altogether, this study shows as proof of principle that conversion of fibroblasts toward a neural cell fate can be achieved solely by small molecule treatment. We identified CB as potent compound to induce neural cell identity and developed a CB-based approach to efficiently generate Schwann cells without any genetic modifications. Compared to existing Schwann cell sources like derivation from pluripotent stem cells (Liu et al., 2012) or as primary cells (Casella et al., 1996), chemical-based conversion is more cost effective and easier to control and to standardize. Because Schwann cells play an important role in development, homeostasis, and diseases of the peripheral nervous system (Bhatheja and Field, 2006), we suggest that iSCs could represent useful tools to analyze Schwann cell functions or pathophysiology in vitro and to develop cellular interaction models allowing to study disease mechanisms in neuron-Schwann cell coculture.

EXPERIMENTAL PROCEDURES

Details are provided as Supplemental Experimental Procedures.

Cell Culture
SCC058 foreskin fibroblasts (Millipore) were seeded in low serum FibroGro (Millipore) containing 1 mM Valproic acid (VPA, Sigma). Cells were treated for 2 days with 1 mM VPA and 6 μg/ml polybrene (Millipore) and subsequently transferred to low attachment plates in NSC medium for sphere formation. After 4 days, spheres were dissociated, and cells were seeded in low attachment plates in NSC medium supplemented with inhibitor mix consisting of 500 ng/ml Noggin (PeproTech), 10 μM SB431452 (Tocris Bioscience), and 1 μM CP21 (Roche, GSK3 inhibitor, published elsewhere). After 3 days, secondary spheres were seeded on polyornithine-laminin (POL)-coated dishes. After attachment (24 hr), medium was replaced with neural differentiation medium. Every other day, 50% of medium was exchanged. For the first 7 days of differentiation, medium was supplemented with inhibitor mix. MACS depletion of CD271-positive cells from the initial fibroblasts was performed using a CD271 Microbead kit (Miltenyi).

For adipocyte and smooth muscle cell differentiation, secondary spheres were plated on growth factor reduced matrigel. After 24 hr, medium was changed to adipocyte differentiation medium. Medium was changed every other day. After 4 weeks, cells were fixed with 4% paraformaldehyde (PFA) and stained with oil red O or anti-SMA.

For chondrogenesis, secondary spheres were cultured as pellet in chondrocyte differentiation medium. After 4 weeks, the pellet was fixed with 4% PFA and analyzed by Alcian blue staining.

Embryonic stem cell-derived neural stem cells (NSCs) were generated as previously described (Chambers et al., 2009). NSCs were cultured on POL in N2B27 supplemented with basic fibroblast growth factor (10 ng/ml), epidermal growth factor (10 ng/ml), and brain derived neurotrophic factor (20 ng/ml).

For iSC/NSC neuron coculture, NSCs were cultured in differentiation medium for 13 days and then seeded in differentiation medium on POL only, fibroblasts, or iSCs at 120,000 NSC-neurons/ 12 well. Fibroblasts and iSCs had been previously labeled with CFSE cell tracker (Invitrogen, 10 μM for 20 min). Every other day, 50% of medium was exchanged. Cells were fixed with 4% PFA at day 13 of coculture.

For iSC/rat DRG coculture, embryonic rat DRG neurons (Lonza) were seeded on poly-D-Lysine-laminin-coated plates and cultured at 37°C, 5% CO_2 in PNGM medium (Lonza) supplemented with 100 ng/ml NGF (PeproTech). To eliminate rat glial cells, cultures were treated with 17.5 μg/ml uridine and 7.5 μg/ml 5-fluoro-2-deoxyuridine (both Sigma) for at least 7 days. Then, iSCs (day 21) were seeded on DRG cultures at 30,000 cells/cm^2. Cultures were maintained in PNGM medium supplemented with 100 ng/ml NGF with 50% medium exchange every other day. At day 4 of coculture, myelination was induced by adding 50 μg/ml ascorbic acid to the medium.

Human primary Schwann cells (Sciencell) were cultured on poly-L-lysine coated dishes in Schwann cell medium (Sciencell).

Kinase Selectivity Profiling
Kinase selectivity profiling was performed using ProfilerPro Kinase Kits from Caliper (PerkinElmer) according to the manufacturer's instructions.

Genome-wide Gene Expression Analysis
RNA samples were processed for microarray expression profiling using the Affymetrix HG-U133_plus_2 platform. Data analysis was performed using Partek Genomics Suite 6.6 (Partek) and Gene Set Enrichment Analysis.

Statistics

Data are presented as mean ± SD. Statistical significance was tested with Student's t test. The number of independent experiments is given as "n."

REFERENCES

Baker, M.D. (2002). Electrophysiology of mammalian Schwann cells. Prog. Biophys. Mol. Biol. 78, 83–103.

Bhatheja, K., and Field, J. (2006). Schwann cells: origins and role in axonal maintenance and regeneration. Int. J. Biochem. Cell Biol. 38, 1995–1999.

Bronner-Fraser, M. (1986). An antibody to a receptor for fibronectin and laminin perturbs cranial neural crest development in vivo. Dev. Biol. 117, 528–536.

Casella, G.T., Bunge, R.P., and Wood, P.M. (1996). Improved method for harvesting human Schwann cells from mature peripheral nerve and expansion in vitro. Glia 17, 327–338.

Chambers, S.M., Fasano, C.A., Papapetrou, E.P., Tomishima, M., Sadelain, M., and Studer, L. (2009). Highly efficient neural conversion of human ES and iPS cells by dual inhibition of SMAD signaling. Nat. Biotechnol. 27, 275–280.

Desban, N., Lissitzky, J.C., Rousselle, P., and Duband, J.L. (2006). alpha1beta1-integrin engagement to distinct laminin-1 domains orchestrates spreading, migration and survival of neural crest cells through independent signaling pathways. J. Cell Sci. 119, 3206–3218.

Ding, J., Yu, J.Z., Li, Q.Y., Wang, X., Lu, C.Z., and Xiao, B.G. (2009). Rho kinase inhibitor Fasudil induces neuroprotection and neurogenesis partially through astrocyte-derived G-CSF. Brain Behav. Immun. 23, 1083–1088.

Dontu, G., Abdallah, W.M., Foley, J.M., Jackson, K.W., Clarke, M.F., Kawamura, M.J., and Wicha, M.S. (2003). In vitro propagation and transcriptional profiling of human mammary stem/progenitor cells. Genes Dev. 17, 1253–1270.

Fernandes, K.J., McKenzie, I.A., Mill, P., Smith, K.M., Akhavan, M., Barnabé-Heider, F., Biernaskie, J., Junek, A., Kobayashi, N.R., Toma, J.G., et al. (2004). A dermal niche for multipotent adult skin-derived precursor cells. Nat. Cell Biol. 6, 1082–1093.

Griffiths, I.R., Dickinson, P., and Montague, P. (1995). Expression of the proteolipid protein gene in glial cells of the post-natal peripheral nervous system of rodents. Neuropathol. Appl. Neurobiol. 21, 97–110.

Groysman, M., Shoval, I., and Kalcheim, C. (2008). A negative modulatory role for rho and rho-associated kinase signaling in delamination of neural crest cells. Neural Dev. 3, 27.

Halfon, S., Abramov, N., Grinblat, B., and Ginis, I. (2011). Markers distinguishing mesenchymal stem cells from fibroblasts are down-regulated with passaging. Stem Cells Dev. 20, 53–66.

Hou, P., Li, Y., Zhang, X., Liu, C., Guan, J., Li, H., Zhao, T., Ye, J., Yang, W., Liu, K., et al. (2013). Pluripotent stem cells induced from mouse somatic cells by small-molecule compounds. Science 341, 651–654.

Huangfu, D., Maehr, R., Guo, W., Eijkelenboom, A., Snitow, M., Chen, A.E., and Melton, D.A. (2008). Induction of pluripotent stem cells by defined factors is greatly improved by small-molecule compounds. Nat. Biotechnol. 26, 795–797.

Jessen, K.R., and Mirsky, R. (2005). The origin and development of glial cells in peripheral nerves. Nat. Rev. Neurosci. 6, 671–682.

Kamholz, J., Sessa, M., Scherer, S., Vogelbacker, H., Mokuno, K., Baron, P., Wrabetz, L., Shy, M., and Pleasure, D. (1992). Structure and expression of proteolipid protein in the peripheral nervous system. J. Neurosci. Res. 31, 231–244.

Kidd, G.J., Ohno, N., and Trapp, B.D. (2013). Biology of Schwann cells. Handb. Clin. Neurol. 115, 55–79.

Ladewig, J., Mertens, J., Kesavan, J., Doerr, J., Poppe, D., Glaue, F., Herms, S., Wernet, P., Kögler, G., Müller, F.J., et al. (2012). Small molecules enable highly efficient neuronal conversion of human fibroblasts. Nat. Methods 9, 575–578.

Lehmann, H.C., Chen, W., Mi, R., Wang, S., Liu, Y., Rao, M., and Höke, A. (2012). Human Schwann cells retain essential phenotype characteristics after immortalization. Stem Cells Dev. 21, 423–431.

Liu, Q., Spusta, S.C., Mi, R., Lassiter, R.N., Stark, M.R., Höke, A., Rao, M.S., and Zeng, X. (2012). Human neural crest stem cells derived from human ESCs and induced pluripotent stem cells: induction, maintenance, and differentiation into functional schwann cells. Stem Cells Transl. Med. 1, 266–278.

McKenzie, I.A., Biernaskie, J., Toma, J.G., Midha, R., and Miller, F.D. (2006). Skin-derived precursors generate myelinating Schwann cells for the injured and dysmyelinated nervous system. J. Neurosci. 26, 6651–6660.

Menendez, L., Yatskievych, T.A., Antin, P.B., and Dalton, S. (2011). Wnt signaling and a Smad pathway blockade direct the differentiation of human pluripotent stem cells to multipotent neural crest cells. Proc. Natl. Acad. Sci. USA 108, 19240–19245.

Pennarossa, G., Maffei, S., Campagnol, M., Tarantini, L., Gandolfi, F., and Brevini, T.A. (2013). Brief demethylation step allows the conversion of adult human skin fibroblasts into insulin-secreting cells. Proc. Natl. Acad. Sci. USA *110*, 8948–8953.

Raivich, G., and Makwana, M. (2007). The making of successful axonal regeneration: genes, molecules and signal transduction pathways. Brain Res. Brain Res. Rev. *53*, 287–311.

Schoenebeck, B., Bader, V., Zhu, X.R., Schmitz, B., Lübbert, H., and Stichel, C.C. (2005). Sgk1, a cell survival response in neurodegenerative diseases. Mol. Cell. Neurosci. *30*, 249–264.

Stuhlmiller, T.J., and García-Castro, M.I. (2012). Current perspectives of the signaling pathways directing neural crest induction. Cell. Mol. Life Sci. *69*, 3715–3737.

Terunuma, A., Limgala, R.P., Park, C.J., Choudhary, I., and Vogel, J.C. (2010). Efficient procurement of epithelial stem cells from human tissue specimens using a Rho-associated protein kinase inhibitor Y-27632. Tissue Eng. Part A *16*, 1363–1368.

Toma, J.G., McKenzie, I.A., Bagli, D., and Miller, F.D. (2005). Isolation and characterization of multipotent skin-derived precursors from human skin. Stem Cells *23*, 727–737.

Tropepe, V., Coles, B.L., Chiasson, B.J., Horsford, D.J., Elia, A.J., McInnes, R.R., and van der Kooy, D. (2000). Retinal stem cells in the adult mammalian eye. Science *287*, 2032–2036.

Tursun, B., Patel, T., Kratsios, P., and Hobert, O. (2011). Direct conversion of C. elegans germ cells into specific neuron types. Science *331*, 304–308.

Vazquez-Martin, A., Vellon, L., Quirós, P.M., Cufí, S., Ruiz de Galarreta, E., Oliveras-Ferraros, C., Martin, A.G., Martin-Castillo, B., López-Otín, C., and Menendez, J.A. (2012). Activation of AMP-activated protein kinase (AMPK) provides a metabolic barrier to reprogramming somatic cells into stem cells. Cell Cycle *11*, 974–989.

Vierbuchen, T., and Wernig, M. (2011). Direct lineage conversions: unnatural but useful? Nat. Biotechnol. *29*, 892–907.